Quantum-Inspired Genetic Programming for Single-End Line-to-Ground Fault Location in Transmission Lines with Resilience to High Impedance Faults

Mohammed H. Al-Qaraghuli
Department of Computer Engineering, Imam Al Adham College, Baghdad. Iraq
mohammed.hameed@imamaladham.edu.iq

Zienab R. Khaleel
Department of Computer Engineering, Imam Al Adham College, Baghdad, Iraq
zainebalani81@imamaladham.edu.iq

Mohamed S. Zaky
Department of Electrical Engineering, College of Engineering, Northern Border University, Arar 1321, Saudi Arabia
mohamed.zaky@nbu.edu.sa (corresponding author)

Mahmoud M. Elgamasy
Electrical Engineering Department, Faculty of Engineering, Menoufia University, Egypt
mahmoud.elgamasy@sh-eng.menofia.edu.eg

Adel M. Sharaf
Sharaf Energy Systems, Inc., Fredericton, Canada
profdramsharaf@icloud.com

Asmaa A. Rady
Electrical Engineering Department, Faculty of Engineering, Damanhour University, Egypt
asmaa.rady@dmu.edu.eg

Received: 4 June 2025 | Revised: 25 July 2025, 24 August 2025, 10 October 2025, and 17 October 2025 | Accepted: 18 October 2025

 DOI: https://doi.org/10.48084/etasr.12363

ABSTRACT

Accurately locating faults in transmission lines remains a major challenge, especially when relying on single-end measurements and the presence of High-Impedance Faults (HIFs), which are often difficult to detect using traditional techniques. This paper presents a fault location determination method for transmission lines based on Quantum-Inspired Genetic Programming (QIGP) that does not require a communication link, using measurements from only one end of the line. Current prediction techniques, such as neural networks and multi-layer regression, often rely on parameter tuning or intricate transformations of predictor or outcome variables, but still fail to deliver highly accurate results. The proposed QIGP model enhances the accuracy of fault location estimation, as seen in internal validation analysis. Genetic programming is used to derive a linear equation that improves the precision of fault location estimation. Quantum computing is leveraged to optimize the choice of top-performing solutions while managing parsimony pressure to minimize solution complexity. The results include various fault distances associated with different inception angles, load angles, and fault resistances.

Keywords-quantum-inspired genetic programming; DFT; transmission lines; fault location; one-terminal measurement; matlab

I. INTRODUCTION

Validating self-healing procedures, including fault isolation and system restoration, enhances power system reliability and sustainability. Phase-to-ground faults are the most common in transmission networks, making an accurate fault distance estimation crucial for timely restoration [1]. Precise fault location reduces repair and outage times, improving the reliability of the grid. Most methods require data from both line ends [2-4], depending on costly communication links. For example, the study in [2] used traveling waves and synchronized voltage data, in [3], PMUs were applied with real-time current and voltage angles, and in [4], voltage profiles were built across multiple sites. These approaches are costly and less effective on long lines. Recent studies use AI methods for this purpose [5-6].

A simpler approach is to estimate the distance from the fault using adaptive, approximate measurements. Since the system parameters vary, adaptability is vital. Mining historical fault data enables pattern recognition, improving accuracy and reliability. Numerous data-driven algorithms exist [7-13]. The studies in [7-9] combined machine learning with wavelet analysis to locate faults in nonhomogeneous lines. A KNN regression model was used in [10], fuzzy logic in [11], and in [12], ACO with self-Encoding Neural Networks (ENN) reduced data dimensionality and extracted natural frequencies, achieving <187 m error and 0.43 s fault detection on a 300 km line. In [13], a hummingbird-inspired algorithm employed axial, diagonal, and omnidirectional flight patterns. In [14], an optimal estimation was performed using the binary bat algorithm. Single-end data combined with predictive techniques show promise [7-13], although accuracy may suffer due to complex transformations, large parameter adjustments, and high computational demand. Conventional Genetic Programming (GP) also faces high costs, premature convergence, and difficulty in reaching global optima [15]. Modified Quantum-Inspired GP (QIGP) maintains diversity and avoids local optima, enabling precise and efficient fault estimation [15]. With the multimodal nature of fault localization, QIGP offers robust single-end solutions capable of detecting high-impedance faults. This motivates a QIGP framework for transmission lines to address the challenge of accurate one-terminal earth fault location independent of fault impedance.

This study introduces a precise, communication-free fault location scheme for transmission lines using QIGP. The modified QIGP identifies fault locations efficiently by preserving diversity and avoiding local optima. It uses sequence components of current and voltage phasors with line parameters as input, optimizing GP through superposition-based fitness, crossover, and mutation to lower costs and prevent premature convergence. A quantum rotational gate exploits qubit-based chromosomes for rapid solutions through linear equations. Replacing conventional statistical methods, QIGP provides a more accurate fault prediction equation while meeting computational demands. Sensitivity analyses and simulations confirm its reliability and effectiveness.

II. TEST SYSTEM

The proposed scheme was tested by simulating a 400 kV, two-terminal, 300 km transmission line in MATLAB/SIMULINK using lumped PI line models. Figure 1 shows the setup, and Table I lists the line parameters. A 400 kV, 50 Hz three-phase source with a 0° load angle and 1250 MVA short-circuit capacity (X/R = 10) is connected to Bus A. Another 400 kV, 50 Hz source with a -15° load angle is connected to busbar B2.

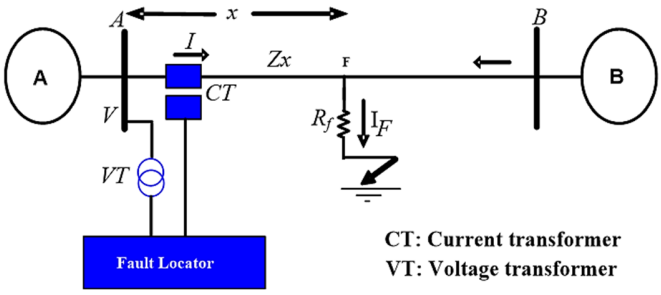

Fig. 1. A schematic diagram for a transmission line subjected to a phase-to-ground fault.

TABLE I. TRANSMISSION LINE VALUES

Component	Parameter	
	Symbol	**Value**
Line	r_1 and r_0	0.0305 and 0.275 Ω/km
	l_1 and l_0	0.9708e-3 and 3.268e-3 H/km
	C_1 and C_0	13e-9 and 5e-9 F/km
Source A	MVASC	50000
	X/R	10
	Angle of EMF	0^0
Source B	MVASC	50000
	X/R	10
	Angle of EMF	-15^0

Various phase-to-ground faults are simulated at different points along the line, with changes in fault resistance, inception angle, and load angle. Three-phase voltage and current samples are taken from one terminal and processed in MATLAB. A 32-sample-per-cycle rate enables accurate power phasor calculation. The recursive Discrete Fourier transform (DFT) extracts the fundamental frequency components at terminal A, which are converted into sequence components for input into the QIGP algorithm. The current and voltage phasors are decomposed into positive, negative, and zero-sequence components using symmetric component transformation [16].

III. THE PROPOSED ALGORITHM

This section describes the proposed QIGP fault location system, designed to derive a precise linear equation for estimating fault distance in transmission lines using single-end measurements. The dataset consists of three-phase voltages and currents, processed into sequence components, with actual fault distances used to evaluate fitness. A normalized Euclidean objective function guides the search, and GP produces an optimal tree representation. By incorporating quantum-inspired principles, the model employs qubit-based chromosomes and probabilistic superposition states, improving diversity and

exploration while running efficiently on classical hardware. Unlike true quantum processors, the framework uses mathematical abstractions of qubits, ensuring accessibility without specialized devices.

GP represents solutions as trees containing terminals and arithmetic functions $F = \{imag, conj, +, -, /, *, abs, angle\}$, enabling flexible symbolic optimization. Quantum rotation gates regulate state transitions, preserving diversity, avoiding premature convergence, and enhancing convergence speed. Through selection, crossover, and mutation, the system iteratively refines equations, achieving accurate and robust fault location predictions.

In the QIGP model, the variable x on the Q-sphere represents a probabilistic state space, allowing superposition and thus broader search exploration compared to classical variables. Quantum rotation gates control rotations along the x, y, and z axes: y-axis transitions prevent early convergence, x-axis adjusts amplitudes to maintain diversity, and z-axis enhances phase alignment for local accuracy. These multidimensional rotations balance exploration and exploitation, refining solutions through genetic operations (selection, crossover, mutation). By leveraging superposition for concurrent evaluations, the model dynamically adapts to trends, improving efficiency and fault location accuracy.

After establishing the initial populations, the subsequent step is to transform the population set through qubit representation. QIGP interprets the quantum state vectors and employs the probabilistic representation of qubits in tree encoding, allowing one tree to represent multiple states in superposition. Quantum rotation gates update this encoding, reducing the risk of premature convergence through quantum crossover, ultimately achieving the optimal solution [17]. QIGP uses qubit-based encoding for the GP population trees, where each internal node can exist in a superposition of n states in the quantum populations but represents only one state when measured in the classical populations. Information about the optimal individuals in each operator or "internal node" guides the application of quantum gates for population updates.

A qubit is the fundamental unit of information in quantum computing. In this context, it represents an eight-state quantum system, defined as follows:

$$|\psi_s\rangle = \alpha_1|000\rangle + \alpha_2|001\rangle + \alpha_3|010\rangle + \alpha_4|011\rangle + \alpha_5|100\rangle + \alpha_6|101\rangle + \alpha_7|110\rangle + \alpha_8|111\rangle \quad (1)$$

$$|\alpha_1|^2 + |\alpha_2|^2 + |\alpha_3|^2 + |\alpha_4|^2 + |\alpha_5|^2 + |\alpha_6|^2 + |\alpha_7|^2 + |\alpha_8|^2 = 1 \quad (2)$$

Operators are encoded using the following values: 000, 001, etc. In QIGP, a multi-qubit is utilized to store and represent a single gene. Each qubit may be in either the '1' state, the '0' state, or a superposition of the two. To be precise, the data expressed by this gene is not stable, but it is still likely. Consequently, when a process is accomplished on this gene, it may be completed simultaneously with all possible information. In this context, each gene contains three qubits. The multi-dimensional unitary transformation is exceedingly challenging to develop. The simple solution is to authorize the binary coding procedure in GP to encode these qubits of multi-states, which involves expanding two qubits to signify multi-states. This method is more straightforward to comprehend and exhibits superior adaptability. To address the challenge of representing multi-state, the proposed system employs the tensor product $\otimes$, which involves the combination of vector spaces to create larger vector spaces. This approach ensures that:

$$|VW\rangle = |V\rangle \otimes |W\rangle = |V\rangle|W\rangle, |101\rangle = |1\rangle \otimes |0\rangle \otimes |1\rangle = |1\rangle|0\rangle|1\rangle \quad (3)$$

As a result, a single gene is represented by three qubits, with each qubit potentially existing in a superposition of two quantum states simultaneously, such as:

$$|\psi_Q\rangle = \gamma|0\rangle + \beta|1\rangle \quad (4)$$

$|0\rangle$ denotes the "turn up" state, whereas $|1\rangle$ represents the "turn down" state. In the general case, multiple qubits are employed to represent the multi-state operator node as follows:

$$q_j^t = \begin{bmatrix} \gamma_{11}^t & \gamma_{12}^t & \cdots & \cdots & \gamma_{1m}^t \\ \beta_{11}^t & \beta_{12}^t & \cdots & \cdots & \beta_{1m}^t \\ \cdots & \cdots & \cdots & \cdots & \cdots \\ \gamma_{k1}^t & \gamma_{k2}^t & \cdots & \cdots & \gamma_{km}^t \\ \beta_{k1}^t & \beta_{k2}^t & \cdots & \cdots & \beta_{km}^t \end{bmatrix} \quad (5)$$

This matrix denotes the chromosome of the t-th generation and the j-th tree in the genetic programming population. The amplitude of a qubit in a superposition state is represented by each element in the matrix, γ or β. The qubit number of the coding state, denoted by k, represents the number of qubits utilized. The operator node number of the tree is denoted by m. This structure enables each "tree" (or solution) in the GP population to simultaneously investigate a spectrum of potential states by allowing a chromosome to contain the superposition for multiple qubits.

Each qubit is initialized to$(\frac{1}{\sqrt{2}}, \frac{1}{\sqrt{2}})$. This demonstrates that a single qubit gene can represent a superposition of all possible states with equal probability. To update the procedure, the Rz quantum rotation gate can be applied [18].

$$Rz(\theta_i) = \begin{bmatrix} 1 & 0 \\ 0 & -1 \end{bmatrix} \quad (6)$$

where $\cup$ denotes an arbitrary single qubit unitary operation, and θ_i represents the rotation angle for each qubit, defined as follows:

$$\theta_i = S(\gamma_m, \beta_m) * \Delta\theta_i \quad (7)$$

where $S(\gamma_m, \beta_m)$ is the sign of θ_i that identifies the direction, and $\Delta\theta_i$ is the magnitude of the rotation gate described in Figure 2. Therefore, γ_m^* and β_m^* are computed as [19]

$$\begin{bmatrix} \gamma_m^* \\ \beta_m^* \end{bmatrix} = \cup(\theta) \begin{bmatrix} \gamma_m \\ \beta_m \end{bmatrix} \quad (8)$$

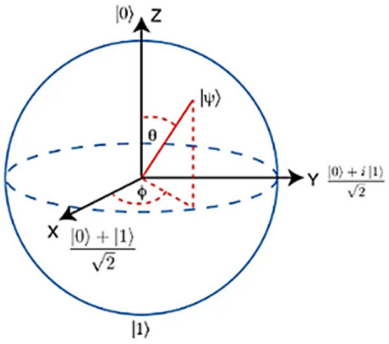

Fig. 2. Bloch sphere.

Finding an objective function is the most difficult part of GP. The surroundings might affect the fitness capacity. In this work, the system utilizes the normalized Euclidean distance metric to identify the most efficient variables that affect the prediction of location, described as

$$f_i = \sqrt[2]{\sum_{i=1}^{n}(|x_{i-}y_i|)^2} \quad (9)$$

where f_i is the computed fitness value, x_i and y_i are the associated result and target, and n is the number of samples. Over successive generations, the solution from each generation gradually converges toward the optimal solution. Figure 3 and Algorithm 1 illustrate the proposed model's stages. The QIGP algorithm begins by initializing with a dataset, the number of generations is set to zero, and a predefined set of arithmetic operators, $F = \{imag, conj, +, -, /, *, abs, angle\}$. An initial population P_{ops} is also set up. The main loop of the algorithm continues while the current generation count t is less than the maximum allowed generations (MAX_GENS). In each generation, t is incremented by one. The current population undergoes Qubit encoding, and a fitness evaluation is conducted to assess each member's performance. The best individuals are then selected for the next population based on their fitness values, and the population is updated using a Q-gate operation. After the Q-gate update, if the termination condition is not met, the algorithm performs crossover and mutation on each member, creating a new population, $New\ P_{ops}$, which replaces the previous one. If the termination condition is met, the algorithm stops and outputs the final population P_{ops} containing the best solution, termed the Best Tree.

The primary parameters employed in the GP process included a population size of 200 individuals, with a total of 2,500 individuals evaluated throughout the procedure. A rotational gate mechanism is used for selection, while mutation is performed using a one-point method and crossover using a two-point method. The generational gap is maintained at 0.5, indicating a 50% turnover rate between generations. Crossover and mutation ratios are both set at 0.5 to ensure equal probabilities for these operations. The termination criterion for the process is defined as a maximum of 200 generations. The parameter values for the QIGP framework, such as population size, mutation rate, and crossover rate, were calculated iteratively by trying numerous configurations to find the best combination. Initially, a range of values for each parameter was determined using insights from similar research and domain experience in genetic programming. These settings were rigorously evaluated on a real dataset to see how they affected the performance of parameters, such as prediction accuracy and computing efficiency. The selection criteria aimed to balance exploration and exploitation, guaranteeing various options while avoiding early convergence. The final values used were those that consistently performed better throughout repeated testing, resulting in accurate fault location forecasts with low computing cost.

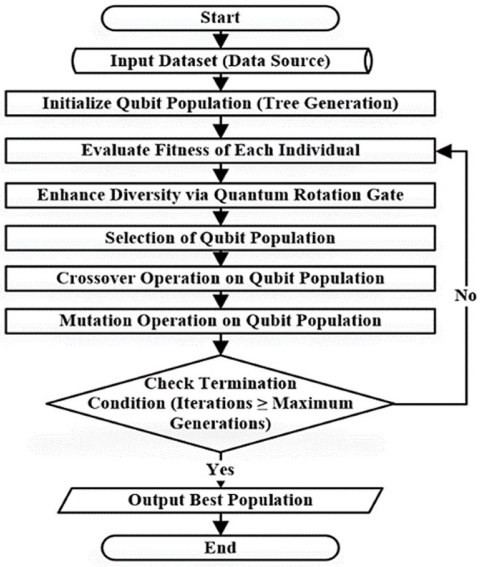

Fig. 3. Prediction model based on QIGP.

```
Algorithm QIGP (T, F, N, G):
P ← InitPopulation (N, F) % random trees /
  individuals
Q ← QubitEncode(P) %
  amplitudes/probabilities per gene
for g = 1...G:
  fit← Evaluate (Q, T) % fitness of each
  individual
  E ← SelectElites (Q, fit) %keep top-k
  Q ← QGateUpdate (Q, E) % rotate angles
  towards elites
  if StopCriterion (fit, g): break
  Off ← [ Mutate (Crossover
   (ParentSelect(Q))) for i in 1...N]
  Q ← Replace (Off, E) %offspring + elites
  (elitism)
return best ← Argmax Fitness(Q)
```

IV. RESULTS AND DISCUSSION

A. The Implementation of QIGP

Extensive tests on a benchmark dataset demonstrate the efficiency of the proposed fault location scheme. QIGP's accuracy is compared with traditional methods, and its adaptability to real-world conditions is shown using various

datasets, including fault data from transmission lines. This study confirms the method's reliability in accurately locating faults without relying on communication channels, using a specific dataset as a case example.

The proposed QIGP system employs Genetic Function Approximation (GFA) to build accurate, flexible models. Unlike traditional regression, GFA evolves model populations from random configurations, enabling the discovery of optimal solutions. The use of both linear and nonlinear functions enhances modeling versatility and accuracy. GFA's ability to generate complex models improves reliability and insight into fault location beyond conventional methods.

QIGP enhances GP by simulating qubit behavior, using superposition, probabilistic state representation, and dynamic rotation angles to efficiently explore solution space on classical computers. Qubit-based encoding preserves diversity and avoids local optima, while a normalized Euclidean distance fitness function improves accuracy. Designed for real-world power transmission, QIGP provides a hardware-independent alternative to quantum computing.

In tests with conventional datasets, QIGP achieved correlation $R > 0.94$, cosine similarity > 0.92, and MSE < 0.09. Figure 4 shows close agreement between predicted and target fault locations. Its quantum-inspired encoding, along with selection, crossover, mutation, and controlled tree depth, sustains diverse solutions and yields precise and flexible fault prediction equations.

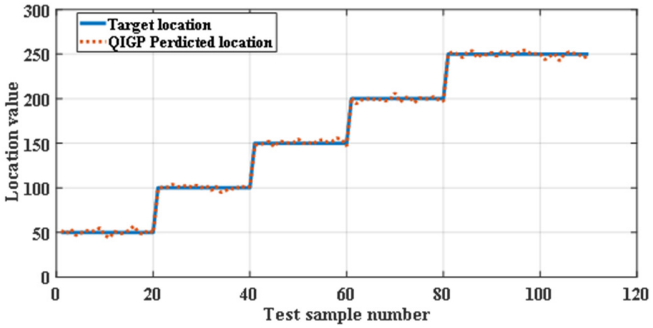

Fig. 4. Experimental (target) versus predicted locations utilizing the QIGP.

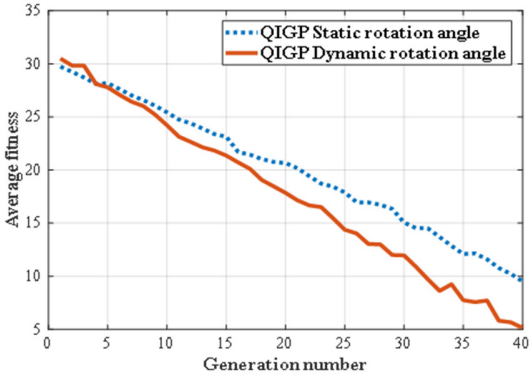

Fig. 5. Evolution of the average fitness in QIGP with fixed and dynamic rotation angles.

Integrating quantum concepts expands the solution space, with quantum chromosomes representing multiple states and rotation gates guiding convergence toward optimal equations. Figure 5 compares fitness across generations, showing that dynamic rotation converges faster and achieves better accuracy than static rotation by adapting during training and avoiding local optima. Hyperparameter tuning—population size, mutation, and crossover rates—further refines performance. Steady crossover enhances recombination, while higher mutation rates expand search, improving adaptability and precision in fault location.

B. Test Results

The proposed fault location scheme was tested on additional simulated faults outside the original dataset, varying in inception angles, fault resistances, and pre-fault load angles. Figure 6 shows consistent accuracy for a 100 km fault across inception angles from 0° to 180°. Figure 7 demonstrates reliable performance at 150 km with fault resistances from 0 to 200 Ω. Figure 8 confirms accuracy for a 250 km fault under pre-fault load angles from 15° to 75°. These results validate the scheme's robustness under varying conditions.

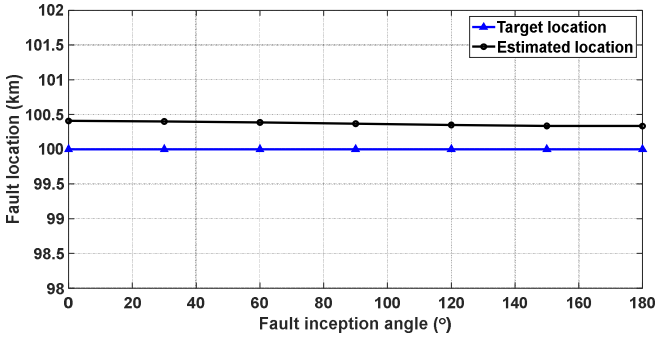

Fig. 6. The output of the proposed scheme under a phase-to-ground fault at 100 km with different inception angles.

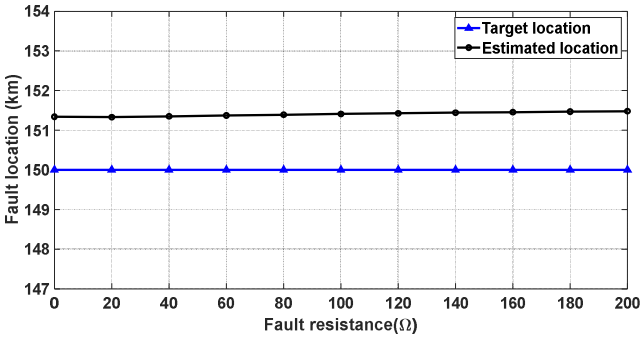

Fig. 7. The output of the proposed scheme under a phase-to-ground fault at 150 km with different fault resistances.

C. Comparison with Previous Works

Fault location techniques in power transmission lines were studied and compared with the previous studies. The comparison was carried out based on three main indicators:

- Indicator 1: The scope of the problem analysis, including Phasor Analysis (Ph), Signal Processing Analysis (SP), and Training and Learning (TL).
- Indicator 2: Specifies the sampling frequency rate in kHz.
- Indicator 3: Represents the maximum error value of the algorithm across all simulation outputs.

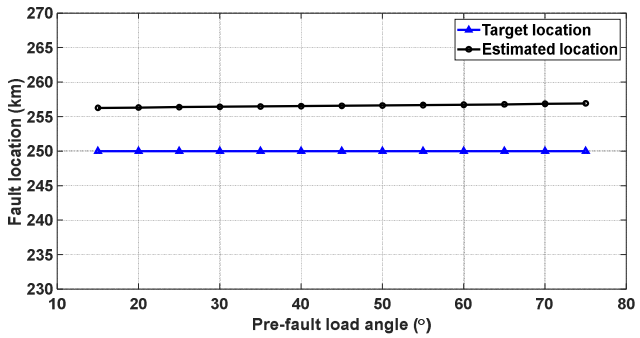

Fig. 8. The output of the proposed scheme under a phase-to-ground fault at 250 km with different load angles.

In [20], a Decision Tree Regression (DTR)-based approach was introduced to estimate the fault distance in double-circuit transmission lines. This method employed single-ended voltage and current measurements and utilized both the DFT and the Discrete Wavelet Transform (DWT) for signal processing. In [21], an algorithm for broken-conductor detection used the charging current characteristics of transmission lines. By analyzing the magnitude and phase angle of the charging current, the method could detect and locate broken conductors using only single-ended measurements. Although effective in preventing reclosing attempts after conductor breakage, its performance was limited to scenarios with measurable charging current and did not address general fault location or classification problems. The algorithm in [22] focused on the detection of open-conductor conditions in systems with unloaded Yg-connected primary transformers. This study recognized that such conditions are difficult to identify due to the lack of abnormal current and voltage signatures. To address this issue, a relaying scheme based on the third harmonic power was introduced, leveraging its dominance in zero-sequence components. However, its applicability remains confined to systems that exhibit specific harmonic characteristics and transformer configurations.

Compared to these studies, the proposed method provides a more generalized and computationally efficient solution that maintains high accuracy under diverse network conditions, without requiring special configurations, complex training, or communication links.

TABLE II. COMPARISON OF THE PROPOSED SCHEME WITH PREVIOUS STUDIES

Ref.	Index 1	Index 2	Index 3
[20]	TL	NA	2.7 %
[21]	Ph	1000	NA
[22]	SP	256	NA
Proposed method	Ph	1.6	2.5 %

V. CONCLUSIONS

This study presents a novel QIGP-based fault location scheme for transmission lines, designed to address several limitations of conventional methods. Unlike regression- and neural network-based approaches, which often depend on extensive parameter tuning and show reduced accuracy under high-impedance faults or diverse operating conditions, the proposed QIGP framework eliminates the need for communication links and provides a precise, communication-free fault location mechanism.

The novelty of this work lies in the integration of quantum-inspired principles—such as qubit-based encoding, dynamic rotation gates, and superposition-driven optimization—into the genetic programming paradigm. This integration preserves population diversity, prevents premature convergence, and enables efficient exploration of the solution space, resulting in more robust and accurate fault location models. Compared to existing schemes, which are typically limited by overfitting or reduced adaptability, QIGP achieves superior performance, with correlation values exceeding 0.94 and a maximum estimation error of only 2.5%. The main contributions of this research are as follows:

- A communication-free framework for single-end fault location, reducing the dependency on synchronized measurements.
- A QIGP-based optimization strategy that leverages quantum-inspired operators to improve convergence speed and accuracy over classical GP.
- Robust performance under diverse scenarios, including varying inception angles, fault resistances, and load conditions, where traditional methods typically degrade.

ACKNOWLEDGMENT

The authors extend their appreciation to the Deanship of Scientific Research at Northern Border University, Arar, KSA for funding this research work through the project number "NBU-FFR-2025-1250-06.

REFERENCES

[1] M. Satea, M. Elsadd, M. Zaky, and M. Elgamasy, "Reliable High Impedance Fault Detection with Experimental Investigation in Distribution Systems," *Engineering, Technology & Applied Science Research*, vol. 14, no. 5, pp. 17248–17255, Oct. 2024, https://doi.org/10.48084/etasr.8292.

[2] Y. Wang and Q. He, "Advanced Identification of Traveling Wave Heads for Transmission Line Fault Localization," in *2025 5th International Conference on Mechanical, Electronics and Electrical and Automation Control (METMS)*, Feb. 2025, pp. 593–597, https://doi.org/10.1109/METMS65303.2025.11048127.

[3] V. Yuvaraju, S. Thangavel, and M. Golla, "Applications of Artificial Intelligence and PMU Data: A Robust Framework for Precision Fault Location in Transmission Lines," *IEEE Access*, vol. 12, pp. 136565–136587, 2024, https://doi.org/10.1109/ACCESS.2024.3464088.

[4] R. Muzzammel, R. Arshad, A. Raza, N. Sobahi, and U. Alqasemi, "Two Terminal Instantaneous Power-Based Fault Classification and Location Techniques for Transmission Lines," *Sustainability*, vol. 15, no. 1, Jan. 2023, Art. no. 809, https://doi.org/10.3390/su15010809.

[5] O. A. Hassen, H. L. Majeed, M. A. Hussein, S. M. Darwish, and O. Al-Boridi, "Quantum Machine Learning for Video Compression: An Optimal Video Frames Compression Model using Qutrits Quantum

Genetic Algorithm for Video multicast over the Internet.," *Journal of Cybersecurity & Information Management*, vol. 15, no. 2, Apr. 2025, Art. no. 43, https://doi.org/10.54216/JCIM.150205.

[6] J. Kh-Madhloom, M. K. A. Ghani, and M. R. Baharon, "Enhancement to the patient's health care image encryption system, using several layers of DNA computing and AES (MLAESDNA)," *Periodicals of Engineering and Natural Sciences*, vol. 9, no. 4, pp. 928–947, Dec. 2021, https://doi.org/10.21533/pen.v9.i4.998.

[7] N. R. Ravesh, N. Ramezani, I. Ahmadi, and H. Nouri, "A hybrid artificial neural network and wavelet packet transform approach for fault location in hybrid transmission lines," *Electric Power Systems Research*, vol. 204, Mar. 2022, Art. no. 107721, https://doi.org/10.1016/j.epsr.2021.107721.

[8] A. R. Adly, S. H. E. A. Aleem, M. A. Elsadd, and Z. M. Ali, "Wavelet packet transform applied to a series-compensated line: A novel scheme for fault identification," *Measurement*, vol. 151, Feb. 2020, Art. no. 107156, https://doi.org/10.1016/j.measurement.2019.107156.

[9] H. A. Jimenez, D. Guillen, R. Tapia-Olvera, G. Escobar, and F. Beltran-Carbajal, "An improved algorithm for fault detection and location in multi-terminal transmission lines based on wavelet correlation modes," *Electric Power Systems Research*, vol. 192, Mar. 2021, Art. no. 106953, https://doi.org/10.1016/j.epsr.2020.106953.

[10] M. Farshad and J. Sadeh, "Accurate Single-Phase Fault-Location Method for Transmission Lines Based on K-Nearest Neighbor Algorithm Using One-End Voltage," *IEEE Transactions on Power Delivery*, vol. 27, no. 4, pp. 2360–2367, July 2012, https://doi.org/10.1109/TPWRD.2012.2211898.

[11] Z. Jiao and R. Wu, "A New Method to Improve Fault Location Accuracy in Transmission Line Based on Fuzzy Multi-Sensor Data Fusion," *IEEE Transactions on Smart Grid*, vol. 10, no. 4, pp. 4211–4220, July 2019, https://doi.org/10.1109/TSG.2018.2853678.

[12] G. Zhang, Q. Zhang, J. Ma, G. Liu, D. Sun, and Z. Zhang, "Fault location of high voltage overhead transmission line based on ACO-ENN algorithm," *International Journal of Critical Infrastructures*, vol. 19, no. 6, pp. 544–557, Jan. 2023, https://doi.org/10.1504/IJCIS.2023.134619.

[13] S. Verma, P. K. Roy, B. Mandal, and I. Mukherjee, "Artificial Hummingbird Algorithm-based fault location optimization for transmission line," *Journal of Engineering and Applied Science*, vol. 71, no. 1, July 2024, Art. no. 149, https://doi.org/10.1186/s44147-024-00475-x.

[14] M. Šipoš, Z. Klaić, E. K. Nyarko, and K. Fekete, "Determining the Optimal Location and Number of Voltage Dip Monitoring Devices Using the Binary Bat Algorithm," *Energies*, vol. 14, no. 1, Jan. 2021, Art. no. 255, https://doi.org/10.3390/en14010255.

[15] P. Fleck, B. Werth, and M. Affenzeller, "Population Dynamics in Genetic Programming for Dynamic Symbolic Regression," *Applied Sciences*, vol. 14, no. 2, Jan. 2024, Art. no. 596, https://doi.org/10.3390/app14020596.

[16] M. A. Elsadd, H. A. Omar, A. R. Adly, and A. F. Zobaa, "Fault-Locator Scheme for Combined Taba-Aqaba Transmission System Based on New Faulted Segment Identification Method," *IEEE Access*, vol. 11, pp. 104270–104284, 2023, https://doi.org/10.1109/ACCESS.2023.3317134.

[17] J. Yang, B. Li, and Z. Zhuang, "Research of Quantum Genetic Algorith and its application in blind source separation," *Journal of Electronics (China)*, vol. 20, no. 1, pp. 62–68, Jan. 2003, https://doi.org/10.1007/s11767-003-0089-4.

[18] A. M. Mohammed, N. A. Elhefnawy, M. M. El-Sherbiny, and M. M. Hadhoud, "Quantum crossover based quantum genetic algorithm for solving non-linear programming," in *2012 8th International Conference on Informatics and Systems (INFOS)*, Giza, Egypt, Feb. 2012.

[19] M. Brezocnik, M. Kovacic, and L. Gusel, "Comparison Between Genetic Algorithm and Genetic Programming Approach for Modeling the Stress Distribution," *Materials and Manufacturing Processes*, vol. 20, no. 3, pp. 497–508, May 2005, https://doi.org/10.1081/AMP-200053541.

[20] A. Swetapadma and A. Yadav, "A Novel Decision Tree Regression-Based Fault Distance Estimation Scheme for Transmission Lines," *IEEE Transactions on Power Delivery*, vol. 32, no. 1, pp. 234–245, Oct. 2017, https://doi.org/10.1109/TPWRD.2016.2598553.

[21] K. Dase, S. Harmukh, and A. Chatterjee, "Detecting and Locating Broken Conductor Faults on High-Voltage Lines to Prevent Autoreclosing Onto Permanent Faults," *in 46th Annual Western Protective Relay Conference,* Spokane, WA, USA, 2019.

[22] X. Wang and W. Xu, "A 3rd Harmonic Power Based Open Conductor Detection Scheme," *IEEE Transactions on Power Delivery*, vol. 36, no. 2, pp. 1041–1050, Apr. 2021, https://doi.org/10.1109/TPWRD.2020.3001075.